



4th International Conference on Tissue Engineering, ICTE2015

## Design and Validation of an Open-Hardware Print-Head for Bioprinting Application

Carmelo De Maria<sup>a</sup>, Laura Ferrari<sup>a</sup>, Francesca Montemurro<sup>a</sup>, Federico Vozzi<sup>b</sup>, Ilenia Guerrazzi<sup>b</sup>, Thomas Boland<sup>c</sup>, Giovanni Vozzi<sup>a,d,\*</sup>

<sup>a</sup>Research Center E. Piaggio University of Pisa, Largo Lucio Lazzarino 1, 56122 Pisa, Italy

<sup>b</sup>Institute of Clinical Physiology National Council of Research, Via Giuseppe Moruzzi 1, 56124 Pisa, Italy

<sup>c</sup>Department of Metallurgical and Materials Engineering University of Texas at El Paso, 500 W. University Ave, El Paso, Texas (US)

<sup>d</sup>Department of Information Engineering University of Pisa, Via Giuseppe Caruso 16, 56122 Pisa, Italy

### Abstract

In the last decades drop-on-demand inkjet technology played an increasing role in industrial and medical applications. This is due to the ability to deposit a small amount of material in precisely defined position. In the field of Biofabrication, inkjet printers are used to build 2D and 3D scaffolds and gels with biological molecules, including living cells. Several works, including seminal papers on inkjet bioprinting, were carried out with modified office printers. These printers have fixed structural characteristics and operating size, especially on the print-head, limiting the range of materials that can be dispensed. The aim of the present work is the design and fabrication of an open-source piezoelectric inkjet print-head, optimized for the bioprinting field. This low-cost, reproducible, reliable, versatile and biocompatible device will enable various research laboratories to work with a shared device; the open source allowing for parts to be modified to suit specific needs. The design was carried out by Finite Element (FE) modelling of the piezoelectric, mechanical, fluid dynamics and their coupling. The design was optimized for shear rate, which we minimized in order to be able to print cells. The mechanical frame of the printer was designed and built using a low-cost 3D printer. The nozzle plate was fabricated from a polycarbonate disc coated with biocompatible silicone, to increase the hydrophobicity of the outer surface of the disc, preventing ink adhesion on the edge of the nozzle; the refilling system, and the electronic control were also part of the project and will be freely available to download. The FE models were validated with ad-hoc experiments, printing water, gelatin solution, and cell culture media, by modulating the wave power in amplitude, frequency and duty cycle. The tests showed a large working window both respect to viscosity and to surface tension. Finally Human Skin Fibroblasts (ATCC-CRL-2522, Teddington UK), suspended in culture media, were printed. Cell viability, assessed by CellTiter-Blue and LIVE / DEAD tests, resulted comparable with the control, demonstrating the validity of the first open source piezoelectric inkjet print-head for biofabrication.

© 2015 Published by Elsevier Ltd. This is an open access article under the CC BY-NC-ND license

(<http://creativecommons.org/licenses/by-nc-nd/4.0/>).

Peer-review under responsibility of IDMEC-IST

**Keywords:** Inkjet; Piezoelectric; Bioprinting; Opensource.

\* Corresponding author. Tel.: +39-050-2217056 ; fax: +39-050-2217051.

E-mail address: [g.vozzi@centropiaggio.unipi.it](mailto:g.vozzi@centropiaggio.unipi.it)

## 1. Introduction

The term inkjet indicates a number of different printing technologies, all of which accomplish the delivering of streams of ink drops, which are deflected onto the substrate, based on data contained in digital files. Inkjet printers can be grouped into two categories: continuous (CIJ) and Drop-on-Demand (DOD). The CIJ printers are based on the Plateau-Rayleigh instability to produce a stream of droplets, of which only a small fraction is used to print. In contrast, the DOD printers allow the formation of drops in response to the activation of a transducer. The most used DOD printers are based on the thermic and the piezoelectric principles, respectively. The high resolution and the ability to eject small volume drops on different types of substrate, without contact and in predefined paths, are the features that enabled DOD technology to expand its application fields, as biology and materials science where many protocols require the ability to deposit small amounts of solutions in predefined position, such as for the fabrication of DNA microarrays [1]. In the field of Biofabrication, inkjet printers have been widely used to spot a gradient of growth factors [2], to print living cells [3], and to build scaffolds [4]. Indeed, using a layer-by layer approach typical of rapid prototyping systems, 2D and 3D well-defined structures have been built using biomaterials, cells and biomolecules for application in tissue engineering and in regenerative medicine [5].

The principle of operation of piezoelectric inkjet system is based on the acoustic wave theory. The electrically induced motion of the piezoelectric crystal compresses the ink in contact with the transducer, forming an acoustic pressure pulse. This pressure interacts with the fluid down to the meniscus at the nozzle. The critical pressure required to form a droplet depends on the rheological properties of the fluid (density, viscosity and surface tension) as well as the geometrical properties of the channel and orifice. Although the operating principle is well known, the process that takes place inside a print head is very complex; its physics and fluid dynamics are still deal of research. The printability of an ink is usually assessed using the Ohnesorge number (or is inverse, the Z number) defined as the ratio of viscous forces over the inertial and surface tension forces [1,6].

As result of this complexity and the necessity of miniaturization, the inkjet printing market is a prerogative of big companies (HP, Canon etc..). Several scientific works, including seminal papers on inkjet bioprinting, were performed with modified office printers. These printers have fixed structural characteristics and operating size, especially on the print-head, narrowing the range of materials that can be dispensed. In order to overcome these limitations, the aim of the present work is the design, fabrication and validation of an open-source piezoelectric inkjet print-head (PIJ), optimized for the bioprinting field. This low-cost, reproducible, reliable, versatile and biocompatible device will enable various research laboratories to work with a shared system; the open source allowing for parts to be modified to suit specific needs. The Finite Element (FE) method, implemented with the software Comsol Multiphysics, guided the design of the device, allowing also the evaluation of important parameters for Bioprinting application. The validation of the PIJ was carried out by printing various fluids, with different nozzles and with different operating conditions, and finally printing a suspension of living cells.

## 2. The Piezoelectric inkjet print-head design and fabrication

### 2.1. Mechanical design

The design of the system was inspired by the Reprappable-inkjet, an open source project hosted by the RepRap.org website, which collects the blueprints of several open 3D printers [7]. The PIJ is composed by the following parts (figure 1a):

- a plastic threaded **central body** and a **plastic cap** screwed on it, which make the external body of the PIJ. These parts were designed to be fabricated by a low cost, open source 3D printer: the .STL files are stored at [8]. No screws are needed to couple the two parts (figure 1b);
- the **chamber**, made of an ad-hoc O-ring (22x1.3 mm), for sealing the interior volume;
- the piezoelectric **actuator** made of a piezo buzzer, a commercial piezoelectric bimorph disc with the brass (27 mm in and 0.22 mm in thickness), on which a piezoelectric disc (20 mm in diameter and 0.23 mm in thickness) was glued. The piezoelectric disc also forms the upper wall of the chamber. The actuator is connected to the electronic circuit with two wires; one soldered oh the PZT disc and the other one on the brass disc;

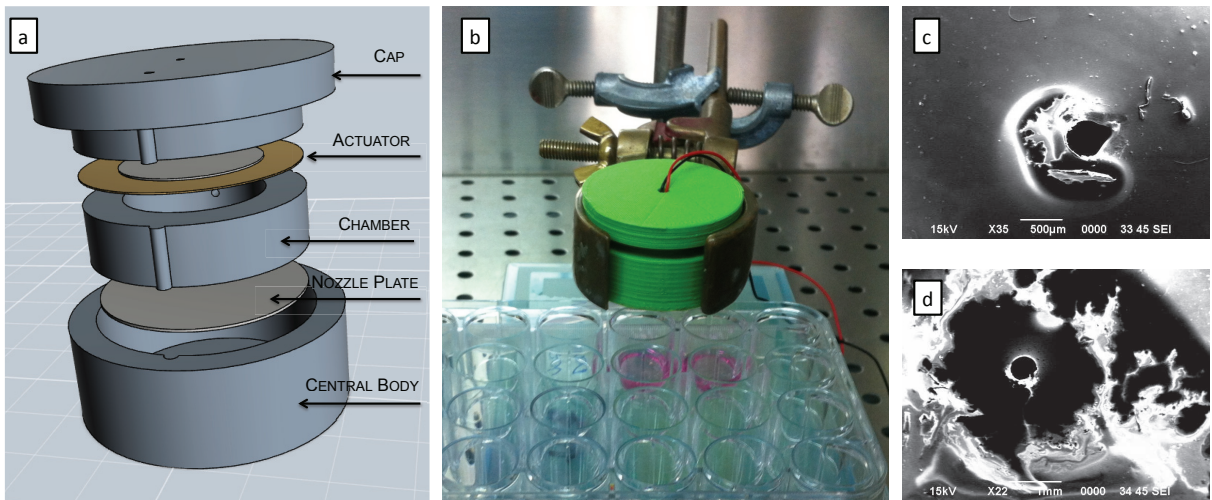


Fig. 1. (a) Exploded drawing of the IPJ; (b) IPJ prototype during cells printing experiments; (c) SEM image of the nozzle plate with silicone polymerized at 60°C; (d) SEM image of nozzle plate with silicone polymerized at room temperature. It is possible to observe the microstructural modification at the nozzle, that obstructs the drop formation.

- the **nozzle plate**, made of a polycarbonate disc coated with silicone (Sylgard<sup>®</sup> 184, Dowcorning, US), for having an hydrophobic outer surface to prevent the adhesion of the ink. The silicone polymerization must be occur at room temperature; otherwise the microstructure of the nozzle can be altered (figure 1c-d). The nozzle orifice was bored by mechanical drills or by an hot wire. The nozzle plate has also a 3 mm hole for the connection to the refill system;
- the **refill system**, made of a reservoir (a commercial syringe) and a soft silicon tube with an inner diameter of 1 mm (not shown in figure 1);

## 2.2. Control

The PIJ is controlled using an Arduino Uno rev3 [9], a low cost and small size electronic board equipped with an ATmega328P micro controller, useful for quickly prototyping. A customized circuit unit was designed in order to have the common ground between the control board and the piezo actuator, but at the same time electrical decoupling. Briefly, a workbench power supply unit, with a range 0-40V, was connected directly to the piezo actuator and to two voltage regulators LM317, properly mounted to set the voltage of the Arduino board to 9V. The Arduino board drives the piezo element through a mosfet (IRF540), which acts as a switch, electrically decoupled from the board by an optocoupler 4N30. In this way the piezo can be controlled with a customizable square wave, whose frequency, duty cycle (DC) and time length, are controlled by Arduino, while the amplitude by the workbench power supply unit. The Arduino board is also connected to computer by an USB board, to allow the user to decide the parameters of the square wave from keyboard, thanks to a purposely developed firmware, using the CmdMessenger Library, and the client PuTTY. The schematic of the electronic board and the firmware for Arduino are stored at [8].

## 2.3. The FE analysis

A multi-physics model was implemented to guide the design of the PIJ, both in terms of size and working parameters. Firstly a parametric simulation of the piezoelectric actuator was performed by varying the stimulation parameters, i.e. amplitude, frequency and DC of the square wave. Then the piezoelectricity equations were coupled to the Navier-Stokes equations, to study the ink flow. The FE models were implemented in the software Comsol Multiphysics (The COMSOL AB, Sweden), using the “Piezoelectric device” and the “Single Phase Flow” modules.

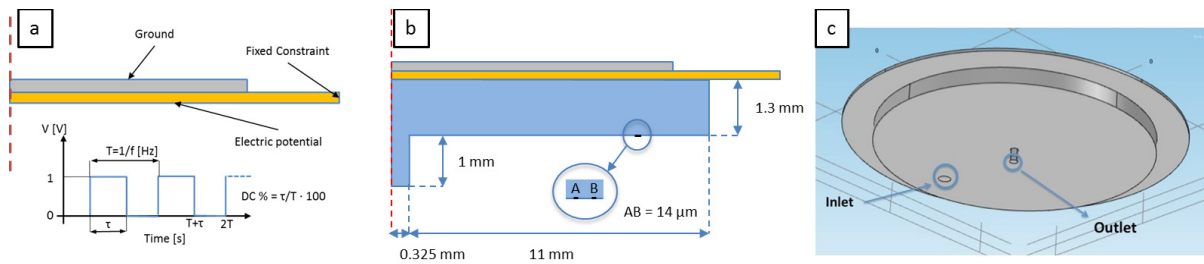


Fig. 2. (a) Geometry of the piezoelectric actuator model. It is possible to note also the boundary conditions, and the parameters of the square wave; (b) 2D axial symmetric geometry of the multi-physics model; (c) 3D geometry of the multi-physics model

### 2.3.1. The piezoelectric actuator

The piezo-electric actuator was modeled into a 2D axial-symmetric workspace with a time-dependent study (figure 2a). The piezoelectric material is the PZT-5H, used in the bend-mode, while the brass disc was defined as an isotropic linear elastic material. The properties of both material were imported from the software library. The boundary conditions, as indicated in figure 2a, are the “Fixed constraint” (i.e. no displacement) at the right end of the brass disc, “Ground” and “Electric Potential” for the upper and lower boundary of the piezo element respectively, and “axial symmetry” for those boundaries on the axis of symmetry. The parametric simulation was carried out by varying the square wave shaped electric potential applied to the piezoelectric material: the amplitude ranged from 20 V to 29 V (with 3 V step), the frequency from 100 Hz to 250 Hz (with 50 Hz step) and the duty cycle was equal to 25, 50 and 75%. The ad hoc mesh discretized the system into 10295 triangles. The maximum element size base is 0.04 mm.

### 2.3.2. Fluid dynamics of the chamber

The fluid dynamics of the chamber is modelled with two simulations, 2D axial-symmetric one and a 3D one (figure 2b-c). In both cases, the fluid inside the chamber, deionized water, is considered incompressible and the flow laminar. Its physical properties were taken from the software library. The piezo actuator has the same parameters indicated in the previous section, for both models. The main difference between the two models is on the simulation of the refill system, which actually is not axial symmetric: in the 2D model it is schematized by a circular crown whose area is equal to the refill hole. The coupling between the motion of the piezo actuator to the ink flow is given by matching the fluid velocity at the upper wall of the chamber to the displacement velocity of the piezo actuator. The refill system was modeled as an inlet, while the nozzle boundary as an outlet. The other boundaries of the chamber have a “no slip” condition. The ad hoc mesh discretized the 2D axial symmetric model into 30874 triangles. A tetrahedral mesh with 974823 elements discretized instead the 3D geometry. The maximum element size base is 0.04 mm.

## 3. Materials and methods

### 3.1. Print head characterization and FEM validation

The working window of the IPJ respect to 3D different inks, deionized water, 0.1% gelatin in deionized water and EMEM Culture medium (without serum), was evaluated modulating the wave power in amplitude [V], frequency [Hz] and Duty Cycle [DC%] in the following ranges: 18-26 V, 50-250 Hz and 25-75% respectively. Three different diameters of the nozzle were tested: 0.5, 0.65 and 0.8 mm. Gelatin from porcine skin and the culture medium were purchased from Sigma Aldrich. After the verification of the drop formation, the quantity of ejected material was evaluated by its weight using an analytical balance (Mettler Toledo AE240). The following parameters were calculated:

- the minimum printing time ( $t_{min}$ , [s]), defined as the time needed to generate a drop, evaluated as the time for which the actuator must be powered on. It was obtained with an iterative approach, decreasing the printing time until no drops are formed;

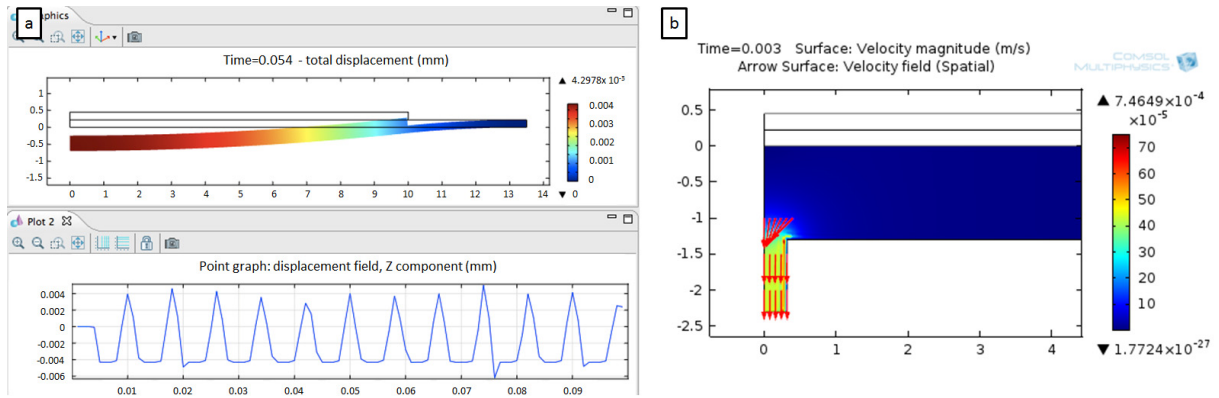


Fig. 3. (a) FE analysis of the actuator: the upper graph shows the deformed shape, while the lower one indicates the bouncing behavior of the piezoelectric disc; (b) fluid dynamics of the inside the IPJ during the printing phase.

- printing resolution, defined as the quantity of ink printed during the minimum printing time and thus expressed as  $g/t_{min}$ ;
- flow rate, evaluated by continuous printing over 5 seconds and expressed as g/s.

Tests were performed in triplicate for each combination (material, printing parameters, nozzle size). Obtained results were used to validate the FEM model, and to choose the best parameters for cell printing (see next section).

### 3.2. Cells printing

BJ Human Skin Fibroblast (ATCC-CRL-2522, Teddington UK), a line of immortalized human fibroblasts, was suspended in EMEM culture medium at a concentration of 100.000 cells/ml and put in the reservoir connected to the IPJ. The following parameters were chosen: nozzle 0.5 mm, DC 50%, voltage 26 V, frequency 166Hz. A total of 360 drops per well (about 5000 cells), for a total volume of 50  $\mu$ l, were printed into a 24-wells multiwell. Each well was previously filled with 450  $\mu$ l of complete medium (EMEM containing 10%v/v Fetal Bovine Serum, 2mM L-glutamine and 1%v/v of antibiotic antimicotic solution), as the impact of the droplet with rigid substrates strongly decreases cell viability [10]. At the end of the printing process, a volume of 50  $\mu$ l was taken from the reservoir as a control, and added with 450  $\mu$ l of complete medium. Cell viability was assessed by CellTiter-Blue<sup>®</sup> Assay [11] and LIVE/DEAD Assay [12]. The CellTiter-Blue Assay is a fluorometric method for valuing cells metabolic capacity as indicator of cells viability. Viable cells retain the ability to reduce the indicator dye (resazurin) into an highly fluorescent product (resofurin ex/em 579nm/584nm). Nonviable cells lose metabolic capacity, do not reduce resazurin, and thus do not generate a fluorescent signal. 50  $\mu$ l of CellTiter-Blue Reagent is added directly to each well, the plate was incubated at 37°C in a humidified, 5% CO<sub>2</sub> atmosphere to allow cells to convert resazurin to resorufin, and after 150min the resofurin emission value was measured. The viability was expressed as % of control. The LIVE/DEAD calcein AM/ethidium homodimer-1 Assay is a method to discriminate viable from nonviable cells. Only viable cells retain the esterase ability to transform calcein AM (nonfluorescent) into calcein (fluorescent ex/em 495nm/515nm). Nonviable cells were stained with Ethidium homodimer-1, a fluorescent dye (ex/em 495/635nm) which bind to nucleic acid only in cells with damaged membranes. Briefly, 4  $\mu$ M EthD-1 and 2.5  $\mu$ M calcein AM in PBS was added at samples and incubated at 37°C for 30 min. All stained samples were imaged using fluorescence microscopy.

## 4. Results and discussion

### 4.1. FE analysis

#### 4.1.1. The actuator

A piezoelectric disc, fixed along the outer perimeter, bends when powered (figure 3a, upper graph). The disc can assume a concave or convex shape, depending on the potential difference, positive or negative, respectively. The FE models show also particular behavior: during the part of the square wave at 0V, the actuator does not return to its rest position, but it deforms in the opposite way (figure 3a, lower graph). As a consequence, this phenomenon allows the spontaneous filling of the chamber, eliminating the need of a bipolar wave, and thus simplifying the power supply circuit. An uncontrolled displacement, however, may result into an air bubble entrance from the nozzle. Simulations indicates, in addition, that the maximum displacement of the piezo actuator increases as the voltage increases.

#### 4.1.2. Fluid dynamic of the chamber

An example of ink flow into the IPJ is provided in figure 3b. The output flow, of both 2D axial symmetric and 3D simulations, was evaluated and the derived values were compared in order to define the error made passing from the 3D geometry to the 2D. The amount of printed material in the interval 12 - 16 ms, calculated by the integration of the flow rate over the time, indicated an average difference of 16%, passing from the 1.698 mg of the 3D model to the 1.429 mg of the 2D axial symmetric one. Nevertheless these differences, these simulations were extremely useful for the estimation of the shear stress, an important parameter during the biofabrication process, because it extremely affects the cell viability. The shear stress is proportional to the velocity gradient at the nozzle: for this reason it is substituted by the shear rate, easier to be calculated. The average shear rate, during the formation of a drop, is given by the ratio between the speed of the droplet [m/s] and its radius [m]. It has been shown that cell death occurs, during printing, under the action of a shear rate  $> 5 \times 10^5$  [1/s] [13]. In our case, the mean velocity, extrapolated from the FE models, and the drop radius, obtained from the experimental tests, discussed in the next paragraph, give a shear rate of  $13 \times 10^3$  [1/s], that should avoid the membrane rupture.

### 4.2. Print head characterization and FEM validation

For each type of nozzle, the printability of each type of ink was firstly checked as a function of the square wave parameters. Taking as example the 0.8 mm nozzle and the deionized water as ink, the printability can be plotted as in figure 4a. In the case of DC 50% the stable stream of drops was observed at 100 and 125 Hz and at 20, 23 and 26 V. For the other two duty cycles, drops generation is insured in a narrower range of values. Within the printability range, generally speaking, the minimum printing time decreases as the wave amplitude increases (figure4b), as a consequence of an higher displacement of the piezo element. It is important to note that to obtain a drop, there is the necessity of more than one cycle of the stimulation (from 2 to 10). However the printing resolution, that is the drop volume printed in the minimum printing time, is approximately constant. As a consequence, the flow rate increases with the increasing of wave amplitude and frequency. The drops deposited in correspondence of a  $t_{min}$  are different than those obtained with the continuous process, in some cases bigger (as it happens with DC 75%) in other smaller (for DC 50%). This is a clear indication that the shape of the square wave affects the chamber filling, which in turns influence the printing procedure. Indeed, as observed from the FE analysis, during the period in which the actuator is not powered, it bends in the opposite direction, rising a depression inside the chamber: this phenomenon can speed up the refilling process or may result in air bubbles, as observed for the DC 25%. The same consideration can be applied to the various nozzles and materials: the drops volumes at selected printing parameters are listed in table 1.

The performed tests indicated that similar working parameters across the various material: the frequency and the duty cycle are strictly related to the geometry of the system: no drops are observed for square wave over 250 Hz, and a duty cycle of 50% usually gives the best results. Furthermore, the chosen piezo element can not be powered over 30V. Generally speaking it is possible to state, as expected [1], a smaller nozzle diameter results into a smaller droplet; the same happens with an increase in viscosity.

The experimental data were used to validate the FE models. The amount of material that is ejected from the nozzle was calculated by integrating the flow rate over a time equal to  $t_{min}$ ; these values were compared with the experimental drop volume. Results indicates, as average a difference 43% respect to the 2D model and 65% respect

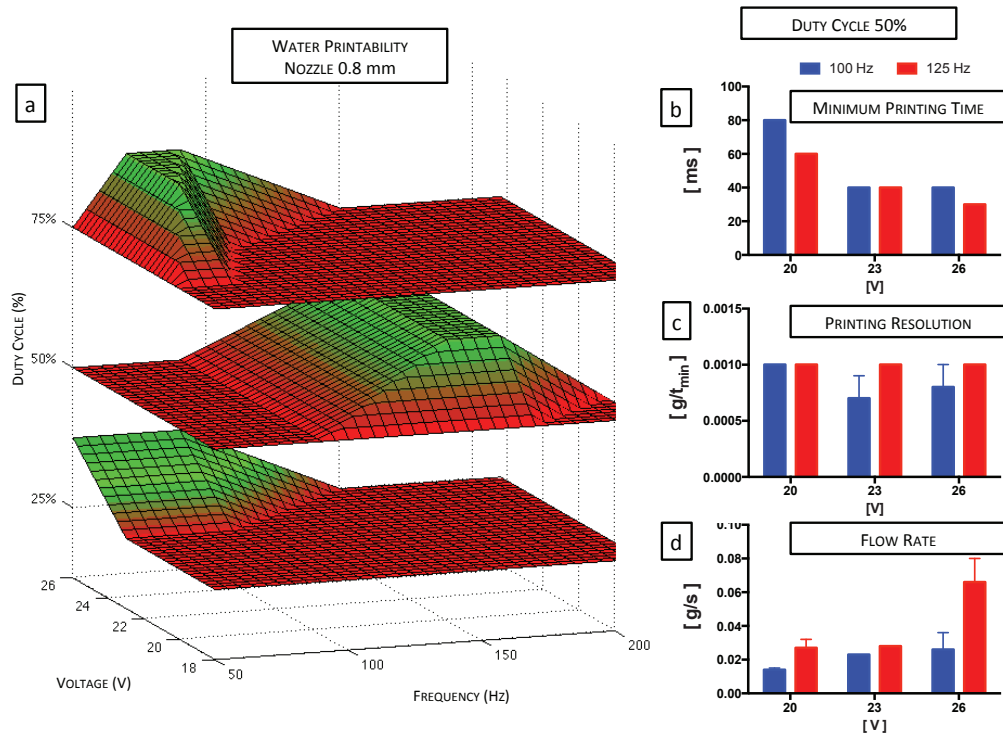


Fig. 4. (a) Deionized water printability for various combination of the printing parameters with a nozzle size of 0.8 mm. The red areas represent a non-printing combination, while in the green ones there is high reproducibility. For DC 50% and two selected frequencies (100 Hz and 125 Hz) in the area of high reproducible printing, (b) the minimum printing time, (c) the printing resolution and (d) the flow rate are graphed.

Table 1. Printing parameters for the tested materials

Material	Nozzle ( $\varnothing$ mm)	Parameters	Drop volume (nl)
Deionized water	0.65	26V - 125Hz - DC 50%	500 $\pm$ 10
	0.80	26V - 125Hz - DC 50%	1000 $\pm$ 10
0.1% Gelatin	0.65	26V - 166Hz - DC 50%	140 $\pm$ 5
Culture Medium	0.5	26V - 166Hz - DC 50%	140 $\pm$ 5
	0.65	26V - 166Hz - DC 50%	160 $\pm$ 5

to the 3D. Several reasons can be addressed: the most important should be the role of the surface tension that is not properly taken into account. In the FE models the entire supplied energy is converted into a continuous stream of fluid that leaves the nozzle.

#### 4.3. Cells printing

The cell culture experiments highlighted the IPJ reduces the cell viability (5a): the reduction can be explained by release of not completely biocompatible components of printing system (such as the brass of the actuator), and less to the printing procedure which induces, as show, a very small stress on cells itself. The remaining printed cells presented a satisfying rate of adhesion (figure 5b), characterized by membrane integrity, confirmed by LIVE/DEAD assay (figure 5c-d): in fact, viable cells are able to bond the Calcein dye (green) of assay, indicating intracellular esterase activity and an intact plasma membrane cell integrity in contrast to Ethidium Bromide (red) dye, useful to show cells under degenerative process. Even so, these results represent an interesting proof of concept and a starting point for the development of this type of printing system.

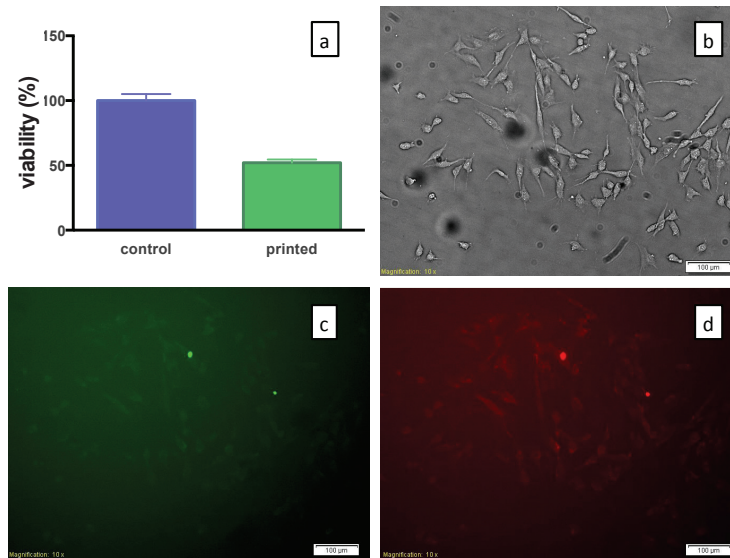


Fig. 5. (a) Cell vitality obtained with the CellTiter-Blue<sup>®</sup> Assay; (b) Bright field image with 10X magnification cells are attached in the well after the printing procedure. (c) red and (d) green channel of the LIVE / DEAD test.

## 5. Conclusion

In the last decades the inkjet technology played an increasing important role in industrial and medical applications, thanks to its ability to generate droplets of extremely small volume that are released without contact on a substrate in predetermined positions. In particular for about ten years the inkjet technology is used in tissue engineering for surfaces functionalization or for controlled deposition of expensive materials. Within this field, the bioprinting of 3D multi-scale and multi-material complex structures has become fundamental. With this background, a piezoelectric, low cost and open source inkjet printhead was designed, fabricated, validated and shared. The project was driven by FE simulations, very useful for estimate printing parameters and to explain experimental results, also if improvements are needed. Biomaterials and living cells were successfully printed. The project is freely available at [8], allowing the various research laboratories to work with a shared and customizable device.

## References

- [1] H. Wijshoff, The dynamics of the piezo inkjet printhead operation, *Physics Reports*, 491 (2010), 77-177
- [2] E.D. Miller, K. Li, T. Kanade, L.E. Weiss, L.M. Walker, P.G. Campbell, Spatially directed guidance of stem cell population migration by immobilized patterns of growth factors, *Biomaterials* 32 (2011) 2775-2785
- [3] T. Xu, J. Jin, C. Gregory, J.J. Hickman, T. Boland, Inkjet printing of viable mammalian cells, *Biomaterials* 26 (2005) 93-99
- [4] C. De Maria, J. Rincon, A.A. Duarte, G. Vozzi, T. Boland, *Polymers for Advanced Technologies* 24 (2013) 895902
- [5] F. Guillemot, V. Mironov, M. Nakamura, Bioprinting is coming of age: report from the International Conference on Bioprinting and Biofabrication in Bordeaux; *Biofabrication* 2 (2010) Editorial.
- [6] B. Derby, Inkjet Printing of Functional and Structural Materials: Fluid Property Requirements, Feature Stability, and Resolution, *Ann. Rev. Mater. Res.* 40 (2010) 395-414
- [7] Reprappable-inkjet [on-line] <http://reprap.org/wiki/Reprappable-inkjet> [verified on April 2015]
- [8] GitHub repository [on-line] <https://github.com/CentroEPIaggio/IPJ-Bio> [verified on April 2015]
- [9] Arduino website [on-line] <http://www.arduino.cc> [verified on April 2015]
- [10] A. Tirella, F. Vozzi, C. De Maria, G. Vozzi, T. Sandri, D. Sassano, L. Cognolato, A. Ahluwalia, Substrate stiffness influences high resolution printing of living cells with an ink-jet system, *Journal of bioscience and bioengineering* 112 (2011), 79-85
- [11] A. Tirella, F. Vozzi, G. Vozzi, A. Ahluwalia, PAM2 (Piston Assisted Microsyringe): A New Rapid Prototyping Technique for Biofabrication of Cell Incorporated Scaffolds. *Tissue Eng Part C Methods*. 17 (2011) 229-37.
- [12] R.E. Saunders, J.E. Gough, B. Derby, Delivery of human fibroblast cells by piezoelectric drop-on-demand inkjet printing. *Biomaterials* 29 (2007) 193-203
- [13] E.Q. Li, E.K. Tan, S. T. Thoroddsen, Piezoelectric Drop-on-Demand Inkjet Printing of Rat Fibroblast Cells: Survivability Study and Pattern Printing. *arxiv.org* (2013) 1310.0656. [verified on April 2015]